Chemosphere 215 (2019) 657–667

Contents lists available at ScienceDirect

Chemosphere

journal homepage: www.elsevier.com/locate/chemosphere

# Assessment on the effects of aluminum-modified clay in inactivating internal phosphorus in deep eutrophic reservoirs

Jingfu Wang [a, *], Jingan Chen [a], Quan Chen [a, b], Haiquan Yang [a], Yan Zeng [a], Pingping Yu [c], Zuxue Jin [c]

[a] State Key Laboratory of Environmental Geochemistry, Institute of Geochemistry, Chinese Academy of Sciences, Guiyang, 550002, PR China
[b] University of Chinese Academy of Sciences, College of Resources and Environment, Beijing, 100049, PR China
[c] College of Resource and Environmental Engineering, Guizhou University, Guiyang, 550025, PR China

## HIGHLIGHTS

- Effects of aluminum-modified clay in inactivating sediment phosphorus were investigated.
- Aluminum-modified clay effectively reduced the release flux of sediment phosphorus.
- Al-P precipitation constituted the main mechanism of the inhibition of sediment P release by aluminum-modified clay.

## GRAPHICAL ABSTRACT

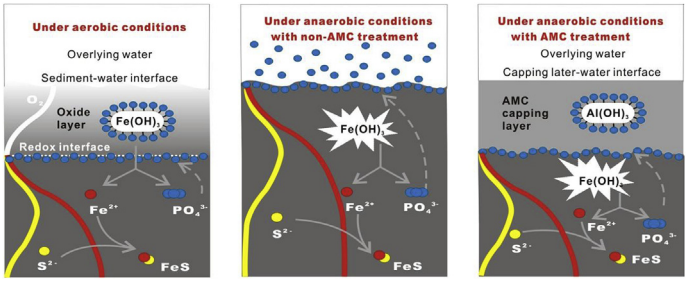


## ARTICLE INFO

*Article history:*
Received 24 July 2018
Received in revised form
21 September 2018
Accepted 16 October 2018
Available online 16 October 2018

*Keywords:*
Aluminum-modified clay
Phosphorus
Sediment
Diffusive gradients in thin films
High-resolution dialysis peeper

## ABSTRACT

Aluminum-salt inactivating agents are extensively applied to the restoration of lakes polluted by internal phosphorus (hereinafter referred to as "P"). However, there is a lack of micromechanism information regarding the sediment P cycle and its interactions with aluminum salts, which has restricted the engineering applications of aluminum salts. In this study, a sediment core incubation system was used to simulate the influence of aerobic and anaerobic conditions on the effectiveness and stability of aluminum-modified clay (AMC). This study also investigated the millimeter-scale dynamics of P across the sediment-water interface (SWI) using the HR-Peeper and DGT techniques. According to the results, sediment P release mainly occurred under anaerobic conditions. When the incubation system was in an anaerobic state, AMC effectively reduced the internal-P loading. In pore water, there was a positive correlation between soluble Fe and SRP, suggesting that the reductive dissolution of Fe-P constituted the main mechanism of sediment P release. After with dosing AMC, the concentrations of SRP and labile P in the capping layer both dropped abruptly to low levels and the content of Al-P in surface sediments rose, suggesting that AMC had strongly adsorbed phosphates, formed inert Al-P and blocked the phosphate exchange between pore water and overlying water. This study elaborated on the micromechanism of the control of sediment internal P input by AMC and revealed that Al-P precipitation constituted the main mechanism of the inhibition of sediment P release by aluminum-salt inactivating agents. The research findings have a great significance for guiding field applications of aluminum-salt inactivating agents.



* Corresponding author.
*E-mail address:* wangjingfu@vip.skleg.cn (J. Wang).

https://doi.org/10.1016/j.chemosphere.2018.10.095
0045-6535/

## 1. Introduction

Eutrophication is a severe challenge worldwide, especially in developing countries. P is generally recognized as a main limiting factor of primary productivity and eutrophication of lakes (Carpenter, 2005). The sources of P in lake water can be classified into two types, namely external P (such as industrial wastewater discharge, domestic sewage discharge and agricultural non-point source pollution) and internal P (P released from sediments). With the continuous strengthening of water environment protection, the input of external P has obviously declined; however, there is already an enormous accumulation of internal P and its contribution to P in lake water is constantly on the rise (Qin et al., 2006; Conley et al., 2009; Nausch et al., 2009; Ding et al., 2018a). For instance, in some lakes, it accounts for as high as 80% of the total P (TP) input (Penn et al., 2000; Søndergaard et al., 2003; Huang et al., 2016). Thus, controlling the release of sediment P into overlying water and reducing the contribution of internal P to P in water are highly important for the prevention and control of lake eutrophication (Chen et al., 2018).

The *in-situ* inactivation technique is a method that is widely used to control the internal P pollution of sediments according to the following principle: by dosing inactivating agents into water, an "inactivation layer" is formed on the sediment surface and the labile P in sediments combines with the inactivating agents (or is absorbed by inactivating agents), thus effectively reducing the release of labile P into overlying water (Rydin and Welch, 1998; Egemose et al., 2009; Malecki-Brown et al., 2009). At present, common inactivating agents include aluminum salts (Reitzel et al., 2005; Huser and Pilgrim, 2014), iron salts (Immers et al., 2014), calcium-rich minerals (Yin and Zhu, 2016; Li et al., 2017; Ding et al., 2018b), zirconium-modified bentonite (Su et al., 2013; Lin et al., 2018), zirconium-modified zeolite (Lin et al., 2019), La-modified bentonite clay (Douglas et al., 1999; Wang et al., 2017; Ding et al., 2018c), and natural soils (Dai and Pan, 2014). Although natural minerals or soils have some effects of inactivating sediment P, their adsorption capacity is much lower than aluminum salts, iron salts and other modified materials. Aluminum salts could hydrolyze in water and generate colloidal, amorphous and highly cohesive $Al(OH)_3$ floccule under the condition of pH 6 to 8, which strongly adsorbs $PO_4^{3-}$ or forms $AlPO_4$ or hydroxyl phosphate $[Al(OH)_y(PO_4)_z]$ precipitation and thus efficiently inhibits sediment P release (Haggard et al., 2005; Lin et al., 2017). As comparing with iron salts, the obvious advantages of aluminum salts is that their inactivation effect is not influenced by redox conditions and that Al-P does not dissolve to release P under anaerobic or even oxygen-free conditions (Cooke et al., 1993). On the contrary, using aluminum sulfate also increases the diffusion rate and diffusion depth of oxygen in sediments (Vopel et al., 2008). However, directly dosing aluminum salts into water may result in chemical pollution, such as excessive Al. In this case, a suitable amount of aluminum salts can be adopted to modify natural minerals, create aluminum-modified inactivating agents and reduce the use rate and environmental risks of aluminum salts. Based on the above considerations, our team has developed an aluminum-modified clay (hereinafter referred to as "AMC") that consists of 30% clay, 15% aluminum sulfate and 55% stone powder. The main components of clay are sodium bentonite and calcium bentonite. The stone powder is carbonate rock produced in Guizhou, and has been grinded to <1 mm. It serves the role of binder in fixing aluminum sulfate and clay together and reduces the loss of inactivating agents at adsorptive sites during the process of water settlement. The production process of the AMC is: firstly, a small amount of water is added to the mixture of clay, aluminum sulfate and stone powder to wet the particles; secondly, the wetting particles are sieved in a small disc and then dried in a high temperature furnace; finally, the dried powder is rotated and screened in the long cylinder.

Understanding the mechanism of inactivation is the premise of rationally utilizing inactivating agents for pollution control. In terms of methodology, some studies adopt centimeter-level sampling methods to explore the relationship between inactivating agents and sediment P composition in samples. However, in engineering applications, the inactivation layer is usually only several millimeters in thickness and it involves competitive adsorption, redox, gradient variations in ion concentrations and other critical processes and information. In this case, it is difficult for these traditional centimeter-level sampling methods, usually with a low spatial resolution, to identify such important micro-scale information. In contrast, emerging *in-situ* passive sampling techniques, including high-resolution dialysis peeper (HR-Peeper), diffusive equilibrium in thin films (DET) and diffusive gradients in thin films (DGT), can quickly identify labile P, labile Fe and sulfides in sediments (Davlson and Zhang, 1994; Xu et al., 2012, 2013). These high-resolution analytical techniques help to reveal the P cycle at the SWI and the mechanism of its interactions with inactivating agents, especially micro-scale processes related to Fe and S cycles (Ding et al., 2012, 2015). Moreover, in engineering applications, the inactivation layer in sediment might be influenced greatly due to the hydraulic or biological turbulence and the settling of particulates in overlying water. These processes also occur in a millimeter or smaller scale at the SWI, further strengthening the necessity using high-resolution sampling techniques in this case.

In this study, parallel sediment core samples collected from the Hongfeng Reservoir, a deep eutrophic reservoir in Southwest China, are used to simulate the internal P input control effect of AMC under aerobic and anaerobic conditions. DGT and HR-peeper techniques are combined with the traditional chemical sequential extraction scheme to determine the chemical compositions, profile distribution and temporal variations in P, Fe and S in sediments and pore water. This study aims to 1) quantify the influence of AMC on internal P input flux and assess the capacity of AMC for immobilizing sediment P; and 2) investigate the influence of AMC treatment on sediment P distribution and elaborate on the possible mechanism of its control over sediment P release.

## 2. Materials and methods

### 2.1. Site description

The Hongfeng Reservoir (26°30′N and 106°23′E) is a deep reservoir built in 1960 in Southwest China. It has a basin area of 1596 $km^2$, a water surface area of 57.2 $km^2$, a maximum water depth of 45 m, a mean water depth of 10.5 m and a total capacity of 601 million $m^3$. The Hongfeng is one of the major drinking water sources for 4.8 million people in Guiyang. In past decades, the basin of the Hongfeng has experienced rapid urbanization and industrialization; as a result, the reservoir has become a P-limited and moderately eutrophic reservoir, whose total N/TP ratio has exceeded 40:1. Hongfeng is a seasonal stratified reservoir and its bottom water is anoxic ($DO < 1\ mg\ L^{-1}$) during the stratification period (from late spring to early autumn). For the rest of the year, the bottom water is aerobic with a mean DO concentration of 6 $mg\ L^{-1}$. In the surface layer (0–5 cm) of the Hongfeng, sediments have a TP content of 766–4306 $mg\ kg^{-1}$ and a mean level of 1815 $mg\ kg^{-1}$ ($n = 107$, dry weight). To be specific, labile P composition content accounts for greater than 50% of the TP (Wang et al., 2015). Due to the sediment P release caused by seasonal anoxia, internal P input has become a major source of P in water (Wang et al., 2016). The water pH of Hongfeng is weakly alkaline, similar to most of the

water bodies in Southwest China.

### 2.2. Sediment incubation and sample collection

In this study, a gravity sampler (11 cm inner diameter) was used to collect four parallel sediment cores in the reservoir. The core samples were immediately sealed in vessels capped with rubber plugs, wrapped with tin foil paper for protection against light and transported to the laboratory within 4 h. At the same time, lake water samples were collected at an interval of 2 m, transported to the laboratory for low-temperature storage (4 °C) and used for chemical analysis or the simulation experiment. To create rational experimental conditions, a multi-parameter water quality monitor(YSI6600V2, YSI Inc., USA) was used on site to monitor the water temperature, dissolved oxygen (DO) and pH of water columns at an interval of 1 m.

The simulation experiment was performed in four groups, namely "anaerobic conditions, dosed with AMC", "anaerobic conditions, not dosed with AMC", "aerobic conditions, dosed with AMC" and "aerobic conditions, not dosed with AMC". In this experiment, the dosage of AMC was 180 g $m^{-2}$ (Fig. S1). The temperature of the incubation system was set at 20 ± 1 °C, which represents the perennial mean temperature of the bottom water in the Hongfeng during the summer. Through injecting continuous and sufficient pure $N_2$ or air, overlying water was controlled at anaerobic(DO < 1 mg $L^{-1}$) and aerobic state(DO > 6 mg $L^{-1}$), respectively. The simulation experiment lasted for a period of 15 d. During the entire incubation process, the sediment cores were kept in darkness.

In the experiment, overlying water samples were collected on the first day at intervals of 0 h, 2 h, 4 h, 8 h and 12 h; from the second day on, they were collected once daily. Because of the high sampling frequency and large cumulative sampling quantity, the same volume of bottom water was replenished after each sampling. In subsequent calculations, these volumes were calibrated. Zr-oxide DGT, ZrO-Chelex DGT and ZrO-AgI DGT were used to determine labile-P, labile-Fe and labile-S at the SWI. HR-Peeper was used to determine soluble P and soluble Fe. Both DGT and HR-Peeper probes were purchased from Easy sensor Ltd. (www.easysensor.net). DGT and HR-Peeper probes were respectively inserted at the SWI of cores and each probe had a segment of no less than 3 cm exposed above the SWI, so as to obtain a complete P concentration gradient at the interface. 48 h after insertion, HR-peeper probes were retrieved and immediately covered with plastic film on the surface to prevent the oxidation of pore water samples. Next, deionized water and wet filter paper were used to clean probe surface and then a syringe was used immediately to transfer the pore water in the chamber into a 0.5 mL centrifugal tube for storage. DGT probes were retrieved 24 h after insertion and cleaned with deionized water. The DGT gel used for 2D analysis was put into a plastic bag for low-temperature storage. For the DGT gel used for 1D analysis, a cutter made of laminated ceramic tips (EasySensor Ltd., Nanjing, China) was used to split binding gel by the interval of 4 mm and the split samples were stored at a low temperature for chemical analysis.

### 2.3. Chemical analysis of DGT/HR-peeper samples

The molybdenum-blue method was used to determine the concentrations of soluble reactive phosphorus (SRP) and TP in overlying water samples (Murphy and Riley, 1962). The 2D labile-P and labile-S concentrations of DGT samples were acquired using the Computer Imaging Densitometry (CID) technique; detailed analysis is described previous reports (Xu et al., 2012, 2013; Ding et al., 2013, 2015). The DGT samples obtained through cutting were dissolved with 1.0 M NaOH and 1.0 M $HNO_3$ for elution in succession. The eluents and the pore water samples collected by HR-peeper were determined by the molybdenum blue method and the phenanthroline colorimetric method to obtain their SRP concentrations and Fe concentrations, respectively (Murphy and Riley, 1962; Tamura et al., 1974).

### 2.4. Determination of sediment properties

After the experiment, the sediments of the 5 cm surface layer were split at an interval of 1 cm. After freeze-drying, the samples were grinded to 100-mesh size for chemical analysis. The TP of the sediments was determined by the $HClO_4$-$H_2SO_4$ digestion method (Frankowski et al., 2002). Sediment P was classified into five forms according to the sequential extraction scheme, including $NH_4C1$-P (loosely sorbed-P), BD-P (mainly consist of iron-bound P (Fe-P)), NaOH-rP (mainly consists of aluminium-bound P (Al-P)), NaOH-nrP (mainly of organic P), HC1-P (mainly of apatite or calcium-bound P (Ca-P)) and Residual-P (mainly of refractory organic-P and inert inorganic-P)(Hupfer et al., 1995; Rydin, 2000). The P concentrations of all extracts were determined by the molybdenum-blue method (Murphy and Riley, 1962).

The geochemical fractions of iron (Fe) in sediments were sequentially extracted based on a five-step method proposed by Tessier et al. (1979). Base on this fractional method, the sediment Fe was divided into five fractions, including exchangeable Fe, carbonate-bound Fe, Fe-Mn hydroxide-bound Fe, organic-bound Fe and residual Fe. Details of extraction processes can be found in several references (Campanella et al., 1995; Xiao et al., 2015).

The Fe, Al, and Ca in sediments were digested with an acid mixture and tested by inductively coupled plasma/optical emission spectrometry (ICP-OES; Vista MPX, Varian, USA). Total organic carbon (TOC) and total sulfur(TS) were determined using an elemental analyzer (VarioMACRO Cube, Elementar, Germany). Before TOC analysis, 1 M HCl was used to remove inorganic carbon from sediment samples.

### 2.5. Calculation of the diffusion flux of P at the SWI

To quantitatively assess the capacity of AMC to immobilize sediment P, the internal P input flux of incubated cores was calculated by two methods, that is, the method based on the variations in the P concentration of overlying water over time and the method based on the P concentration gradient at the SWI and Fick's first law.

Firstly, the sediment P release rate (mg $m^{-2}$ $d^{-1}$) is calculated through linear variation of P concentrations in the overlying water along with time and the surface area of the incubation system (Fisher and Reddy, 2001; Gao et al., 2015), as follows:

$$F = [V(C_n - C_0) + \sum_{j=1}^{n} V_{j-1}(C_{j-1} - C_a)]/ \quad (1)$$

where $F$ is the sediment P release rate (mg $m^{-2}$ $d^{-1}$); $V$ is the volume of the overlying water in the sediment column (L);$V_{j-1}$is the volume of the water sample (L) taken at j-1 time; $C_0$, $C_n$ and $C_{j-1}$are the P concentrations (mg $L^{-1}$) of the water samples taken at the 1st, nst, (j-1)$^{st}$ time; $C_a$ denotes the P concentration of the replenished water (mg $L^{-1}$); $A$ is the surface area of the sediment ($m^2$); and t is the temporal cycle (d). In the calculation, the influence of the dilution effect of replacement water needs to be considered.

Secondly, the internal P influx of lakes can be quantitatively calculated through pore water P concentration profiles at the SWI (Lavery et al., 2001; Yu et al., 2017). In the non-steady-state

diffusion process of sediment, the changing rate of P concentrations over time equals the negative value of the change rate of the diffusion flux with distance. According to the Fick's first law, the P diffusion flux through the SWI can be expressed as Eq. (2)(Ullman and Aller, 1982):

$$F = \phi \times D_s \frac{\partial C}{\partial Z}|_{z=0} \quad (2)$$

where $F$ is the release flux (mg $m^{-2}$ $d^{-1}$); $\phi$ is the porosity of surface sediment; $D_s$ is the effective diffusion coefficient of ions in sediment, where the diffusion coefficient of phosphates can be calculated through empirical formulas and calibrated with temperature and pressure (Li and Gregory, 1974); $\frac{\partial C}{\partial Z}$ is the concentration gradient with a linear change in the P concentration near the SWI, which is usually designated as the spatial range of several to dozens of millimeters above and beneath the SWI.

### 2.6. Statistical analysis

The data shown in this study are represented as the means and standard deviation of three replicates. Pearson correlation analysis was used to examine the correlation between pore water SRP and soluble Fe in sediments with and without inactivating agents. All the statistical analyses in this study were performed by employing SPSS 13.0 (SPSS, USA).

## 3. Results

### 3.1. Effects of AMC on water chemistry in the overlying/pore waters

According to Fig. 1, the hypolimnion in the Hongfeng was anoxic (DO < 1 mg $L^{-1}$) and the concentrations of TP (0.148 mg $L^{-1}$) and SRP (0.106 mg $L^{-1}$) in bottom water were both far higher than their concentrations in overlying water columns (mean: TP 0.039 mg $L^{-1}$; SRP 0.035 mg $L^{-1}$), suggesting that sediments had experienced an intense P release into overlying water under anoxic conditions. The water pH of Hongfeng ranged from 7.6 to 8.4, which gradually decreased with the increasing depths. Therefore, the pH near the sediment-water interface is about 7.6. Fig. 2 shows the SRP concentration of overlying water and the removal rate of SRP from overlying water in the core incubation. Under the condition of DO < 1 mg $L^{-1}$, the SRP concentration of overlying water in the control group gradually rose up from 0.025 mg $L^{-1}$ at the beginning to 0.410 mg $L^{-1}$ on the seventh day, after which it tended to be stable. In a core dosed with AMC, the SRP concentration of overlying water did not experience any obvious increase and the absolute SRP concentration (mean: 0.041 mg $L^{-1}$) was significantly lower than that of the control group (mean: 0.424 mg $L^{-1}$). Under anaerobic conditions, the average removal rate of SRP by AMC reached 90.31% (Fig. 2a). Under the condition of DO > 6 mg $L^{-1}$, whether dosed with AMC or not, the SRP concentration of overlying water always maintained a low level (<0.02 mg $L^{-1}$) or even presented a slightly declining trend (Fig. 2b), suggesting that aerobic conditions had effectively inhibited sediment P release and also promoted the sedimentation of SRP in overlying water.

Table S1 shows the variations in the $Al^{3+}$, $Ca^{2+}$ and $SO_4^{2-}$ concentrations of overlying water and sediment pore water during the incubation experiment. In a core dosed with AMC, no matter under the condition of DO < 1 mg $L^{-1}$ or DO > 6 mg $L^{-1}$, the $Al^{3+}$ and $SO_4^{2-}$ concentrations of overlying water both notably rose from ~8.4 mg $L^{-1}$ to ~23.0 mg $L^{-1}$ (increased to 2.7 times) and from ~46.6 mg $L^{-1}$ to ~123.2 mg $L^{-1}$ (increased to 2.6 times), respectively. The $Al^{3+}$ and $SO_4^{2-}$ concentrations of pore water also rose from ~18.4 mg $L^{-1}$ to ~43.3 mg $L^{-1}$ (increased to 2.4 times) and from ~66.9 mg $L^{-1}$ to ~170.9 mg $L^{-1}$ (increased to 2.6 times), respectively. The results suggested that some aluminum salts in the inactivating agents had dissolved, giving rise to the increase of the $Al^{3+}$ and $SO_4^{2-}$ concentrations of water and pore water. In the presence and absence of AMC, overlying water and pore water did not experience any obvious variation in $Ca^{2+}$ concentration (Table S1).

### 3.2. Effects of AMC on soluble P/labile P in the pore water

Fig. 3a–d shows the concentrations of soluble P and labile P in the overlying water-sediment profiles under different treatment conditions. Under the condition of DO < 1 mg $L^{-1}$, the mean soluble P concentration in the entire profile of the control group not dosed with AMC was 0.235 mg $L^{-1}$, which was significantly higher than that of the experimental group dosed with AMC (0.120 mg $L^{-1}$) (Fig. 3a). At the SWI, the soluble P concentration of the experimental group dosed with AMC was 0.048 mg $L^{-1}$, which was significantly lower than that of the control group not dosed with AMC (0.229 mg $L^{-1}$). The labile P in profiles also presented similar concentration distribution characteristics, especially at the SWI. The mean labile P concentration of overlying water in the control

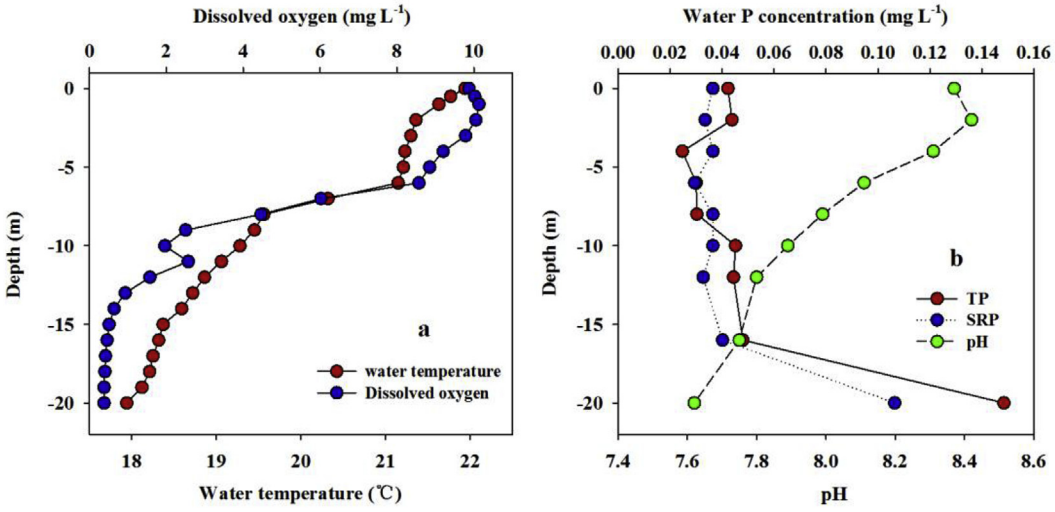


**Fig. 1.** The variations of water temperature, dissolved oxygen (a), SRP, TP and pH (b) with depth in the water column of sampling site in Hongfeng Reservoir (May 25, 2018).

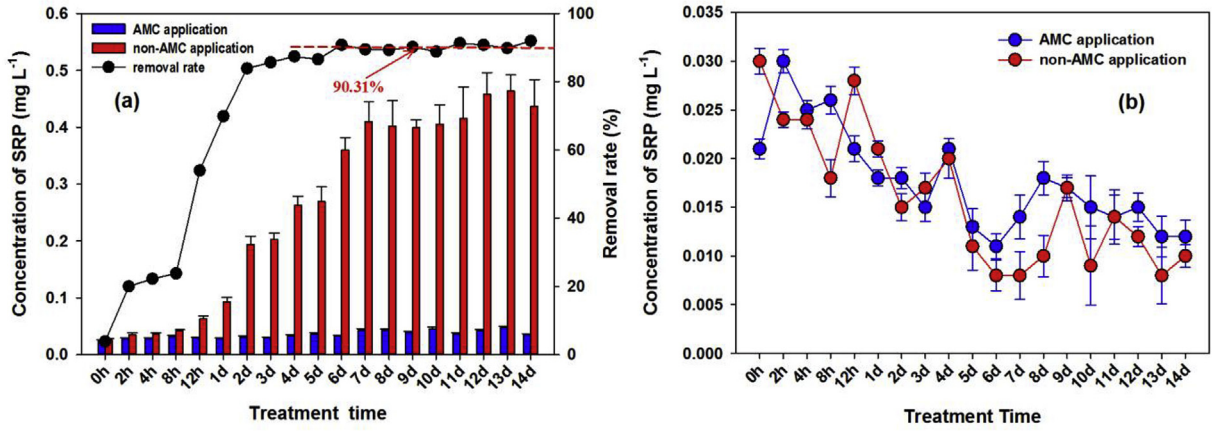


**Fig. 2.** The concentration of SRP in the overlying water and its removal rate under DO < 1 mg $L^{-1}$ (a) and DO > 6 mg $L^{-1}$ (b) conditions. The red dotted line shows the mean value of the removal rate. (For interpretation of the references to color in this figure legend, the reader is referred to the Web version of this article.)

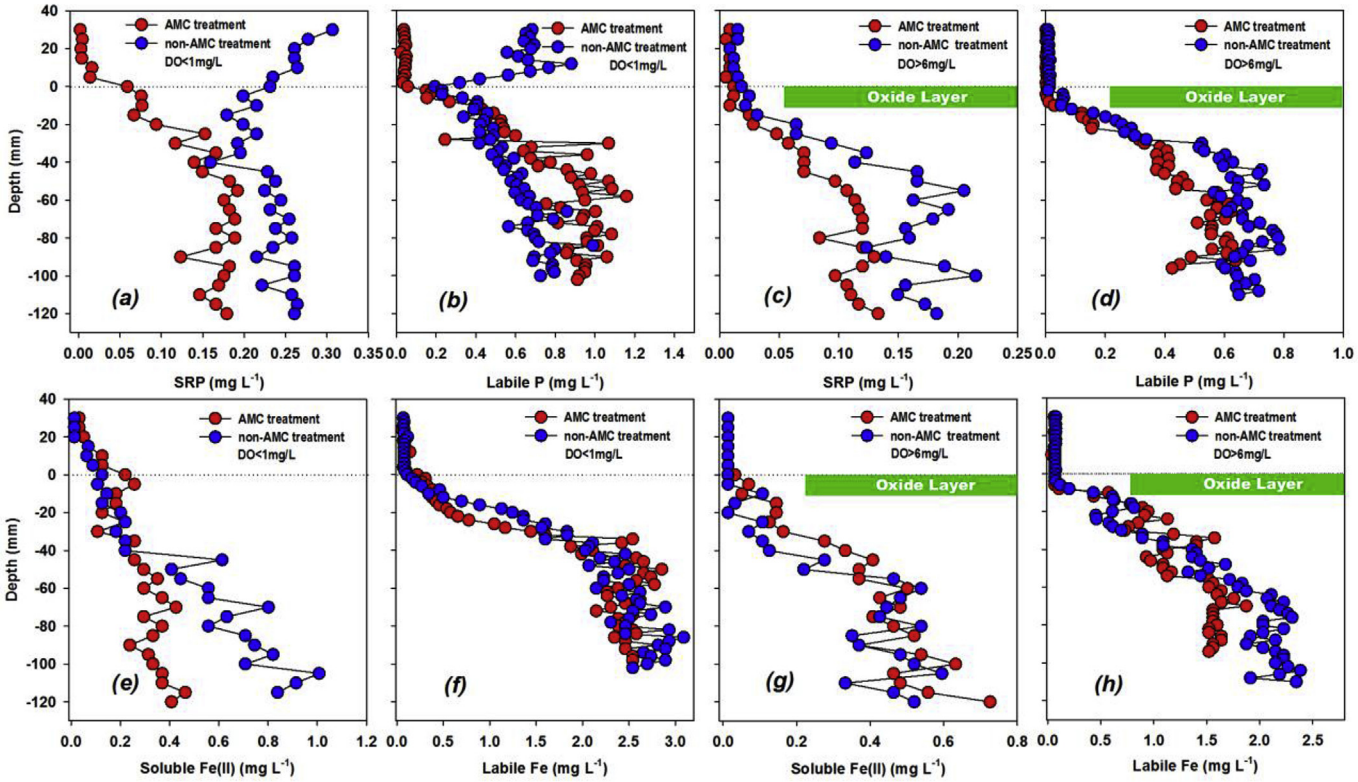


**Fig. 3.** Variations of SRP, labile P measured by HP-Peepers (a,c) and DGT (b,d) and soluble Fe, labile Fe measured by HP-Peepers (e,g) and DGT (f,h) with depths in non-AMC application and post-AMC application sediments at the end of experiment. The location of the sediment-water interface is represented by zero.

group not dosed with AMC reached as high as 0.604 mg $L^{-1}$, which was 14.8 times of that in the experimental group dosed with AMC (Fig. 3b). Under the condition of DO > 6 mg $L^{-1}$, irrespective of AMC dosage, the mean soluble P and labile P concentrations (0.016 mg $L^{-1}$ and 0.025 mg $L^{-1}$, respectively) in the oxide layer (0–10 mm) of the sediment surface were both far lower than their concentrations under the condition of DO < 1 mg $L^{-1}$ (0.143 mg $L^{-1}$ and 0.249 mg $L^{-1}$, respectively). Below the oxide layer (>10 mm), sediments still presented high soluble P and labile P concentration gradients which increased with depth. In the control group not dosed with AMC, the mean soluble P concentration in the entire profile was 0.131 mg $L^{-1}$, which was still higher than that of the experimental group dosed with AMC (0.084 mg $L^{-1}$) (Fig. 3c). The labile P in profiles also presented similar concentration distribution characteristics(Fig. 3d). To sum up, in the sediment incubation experiment, the concentrations of soluble P and labile P under aerobic incubation conditions were significantly lower than their concentrations under anaerobic incubation conditions. Under anaerobic conditions, AMC presented a stronger capacity for inhibiting internal P release.

The 2D measurement of labile P presented a trend similar to that presented by 1D measurement (Fig. 4a–d). Under both aerobic and anaerobic conditions, the labile P concentrations of overlying water and the upper sediment layer in the control group not dosed with

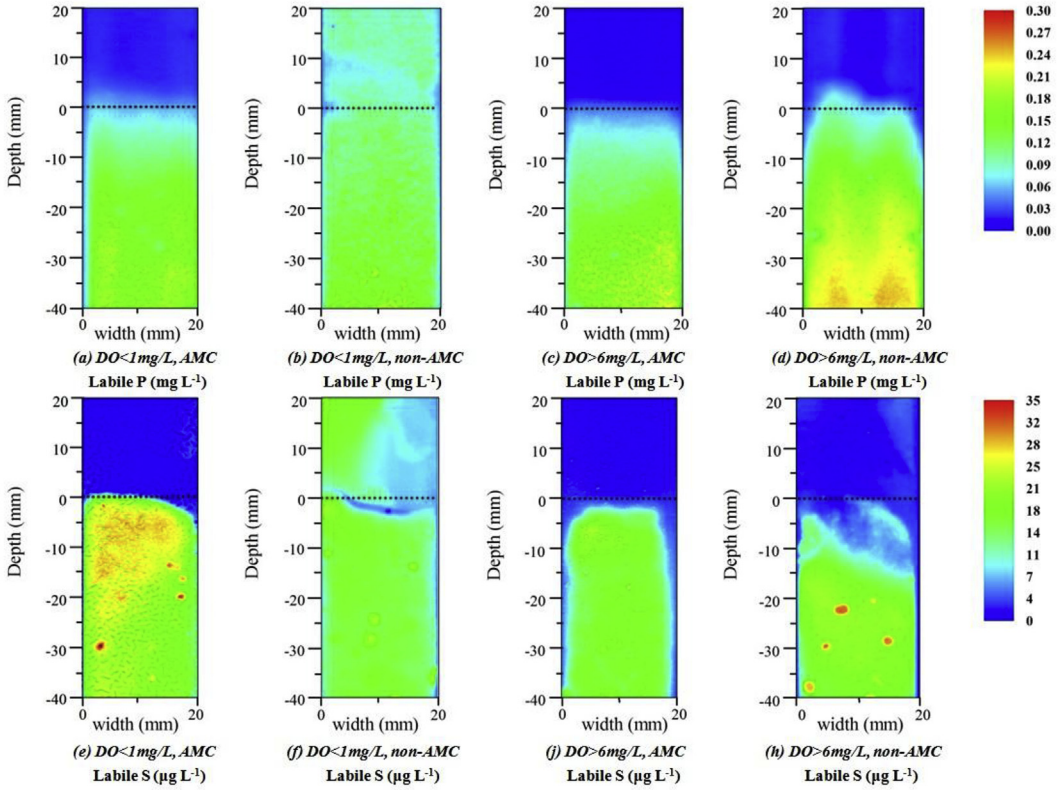


**Fig. 4.** Two-dimensional changes of labile P and labile S concentration in sediment-overlying water profiles, treated (a,c,e,j) and untreated (b,d,f,h) with AMC. The location of the sediment-water interface is represented by zero.

AMC were both relatively high. In the experimental group dosed with AMC, the labile P concentrations of overlying water and the upper 40 mm sediment layer declined to a low level.

### 3.3. Effects of AMC on soluble Fe/labile Fe and labile S in the pore water

Fig. 3e–h shows the concentrations of soluble Fe and labile Fe in the overlying water-sediment profiles under different treatment conditions. Under the condition of DO < 1 mg $L^{-1}$, the soluble Fe concentration of the profile in the experimental group dosed with AMC slowly rose from 0.02 mg $L^{-1}$ (at 20 mm of overlying water) to 0.41 mg $L^{-1}$ (at 120 mm of lower sediments). The soluble Fe concentration of the control group profile not dosed with AMC first increased slowly from 0.01 mg $L^{-1}$ (at 20 mm of overlying water) to 0.22 mg $L^{-1}$ (at 40 mm of upper sediments) and then rose rapidly to 1.29 mg $L^{-1}$ (at 120 mm of lower sediments) (Fig. 3e). Under the condition of DO < 1 mg $L^{-1}$, both with and without AMC dosage, the labile Fe concentrations of the overlying water-sediment profiles uniformly presented similar distribution characteristics, that is, rising rapidly from to 0.08 mg $L^{-1}$ (at the SWI) to 2.20 mg $L^{-1}$ (at a depth of about 40 mm), followed by small fluctuations extending to the profile bottom (Fig. 3f). Under the condition of DO > 6 mg $L^{-1}$, both with and without AMC dosage, the mean soluble Fe and labile Fe concentrations of overlying water were both extremely low (soluble Fe: 0.01 mg $L^{-1}$; labile Fe: 0.08 mg $L^{-1}$). In the oxide layer (0–10 mm), mean soluble Fe and labile Fe concentrations were low as well (0.048 mg $L^{-1}$; 0.159 mg $L^{-1}$), i.e., lower than those of the same layer under the condition of DO < 1 mg $L^{-1}$ (0.173 mg $L^{-1}$; 0.282 mg $L^{-1}$). Below the oxide layer (>10 mm), the experimental group dosed with AMC and the control group not dosed with AMC were highly similar in terms of soluble Fe concentration and distribution, that is, rising gradually from 0.10 mg $L^{-1}$ (at the SWI) to about 0.50 mg $L^{-1}$ (at a depth of about 120 mm) (Fig. 3g). The profile variation characteristics of labile Fe in sediments were similar to those of soluble Fe, that is, in overlying water and the oxide layer (0–10 mm), the labile Fe concentration maintained a low level. Below the oxide layer (>10 mm), the labile Fe concentration rose rapidly from 0.34 mg $L^{-1}$ to 2.23 mg $L^{-1}$ (at a depth of 110 mm) (Fig. 3h).

Fig. 4e–h shows the 2D concentrations of labile S in the overlying water-sediment profiles under different treatment conditions. Under the condition of DO < 1 mg $L^{-1}$, the mean labile S concentration of overlying water in the control group not dosed with AMC was 11.09 μg $L^{-1}$. The mean labile S concentration of overlying water in the experimental group dosed with AMC was lower than the detection limit or 0 (Fig. 4e and f), suggesting that AMC had powerfully inhibited the release of dissolved sulfur in sediments. Under the condition of DO > 6 mg $L^{-1}$, the mean labile S concentration of overlying water in the control group not dosed with AMC was 1.49 μg $L^{-1}$, which was obviously lower than that under anaerobic incubation conditions, suggesting that a high DO concentration could inhibit the release of dissolved sulfur in sediments. Similar to the results observed under anaerobic incubation conditions not dosed with AMC, under the condition of DO > 6 mg $L^{-1}$, the mean labile S concentration of overlying water in the experimental group dosed with AMC was at a low level (0.65 μg $L^{-1}$), but slightly higher than that under anaerobic incubation conditions.

### 3.4. Effects of AMC on sediment properties

Table 1 shows the contents of the main components (TOC, TS, Fe,

**Table 1**
The chemical properties (mean ± SD) of sediments, treated and untreated with AMC, under high and low dissolved oxygen conditions.

| Samples | Depth (cm) | TOC (%) | TS (%) | Al (g kg$^{-1}$) | Ca (g kg$^{-1}$) | Fe (g kg$^{-1}$) | Exc.–Fe (g kg$^{-1}$) | Ca-Fe (g kg$^{-1}$) | Fe/Mn-Fe (g kg$^{-1}$) | Org-Fe (g kg$^{-1}$) | Residual-Fe (g kg$^{-1}$) | Sorbed-P (mg kg$^{-1}$) | Fe-P (mg kg$^{-1}$) | Al-P (mg kg$^{-1}$) | Org-P (mg kg$^{-1}$) | Ca-P (mg kg$^{-1}$) | Residual-P (mg kg$^{-1}$) |
|---|---|---|---|---|---|---|---|---|---|---|---|---|---|---|---|---|---|
| Untreated with AMC & DO < 1 mg L$^{-1}$ | −1 | 6.24 ± 0.22 | 1.73 ± 0.09 | 77.1 ± 6.0 | 58.2 ± 2.7 | 43.2 ± 3.2 | 0.001 | 1.21 ± 0.05 | 27.5 ± 4.2 | 0.68 ± 0.05 | 12.4 ± 1.08 | 11.2 ± 1.5 | 312.6 ± 24.1 | 580.9 ± 30.0 | 42.6 ± 10.3 | 183.7 ± 10.1 | 338.3 ± 14.1 |
| | −2 | 5.91 ± 0.15 | 1.61 ± 0.11 | 52.5 ± 5.5 | 39.5 ± 0.8 | 47.9 ± 2.1 | – | – | – | – | – | 12.0 ± 2.9 | 328.2 ± 20.5 | 603.4 ± 21.1 | 140.2 ± 11.2 | 210.1 ± 16.4 | 363.6 ± 16.5 |
| | −3 | 6.25 ± 0.41 | 1.89 ± 0.06 | 65.7 ± 2.3 | 38.2 ± 1.7 | 26.8 ± 2.3 | – | – | – | – | – | 7.8 ± 2.2 | 335.2 ± 19.2 | 657.2 ± 42.4 | 78.7 ± 7.1 | 208.3 ± 9.9 | 381.1 ± 22.9 |
| | −4 | 5.28 ± 0.32 | 1.39 ± 0.02 | 53.4 ± 1.6 | 30.6 ± 2.4 | 34.3 ± 4.7 | – | – | – | – | – | 10.9 ± 3.4 | 245.1 ± 5.9 | 643.1 ± 25.2 | 91.2 ± 20.6 | 191.3 ± 11.5 | 360.1 ± 13.5 |
| | −5 | 5.46 ± 0.11 | 1.42 ± 0.08 | 106.7 ± 7.8 | 27.8 ± 2.2 | 53.2 ± 1.6 | – | – | – | – | – | 10.7 ± 1.8 | 336.8 ± 30.6 | 588.2 ± 33.3 | 87.5 ± 15.4 | 187.3 ± 6.3 | 390.1 ± 18.3 |
| Treated with AMC & DO < 1 mg L$^{-1}$ | −1 | 6.30 ± 0.24 | 1.43 ± 0.07 | **97.6 ± 4.6** | 56.1 ± 3.2 | 36.5 ± 3.3 | 0.001 | 0.26 ± 0.02 | 26.4 ± 3.0 | 0.52 ± 0.04 | 11.4 ± 0.75 | 12.4 ± 1.1 | 321.1 ± 10.3 | **502.7 ± 24.9** | 47.3 ± 8.1 | 169.3 ± 6.7 | 276.8 ± 18.8 |
| | −2 | 6.42 ± 0.31 | 1.56 ± 0.06 | 67.4 ± 5.1 | 67.4 ± 4.5 | 39.5 ± 2.0 | – | – | – | – | – | 8.9 ± 3.0 | 303.6 ± 11.1 | 415.9 ± 16.6 | 114.2 ± 26.2 | 177.7 ± 11.2 | 335.7 ± 10.7 |
| | −3 | 6.31 ± 0.29 | 1.49 ± 0.03 | 79.1 ± 3.2 | 43.9 ± 1.6 | 41.4 ± 1.9 | – | – | – | – | – | 9.4 ± 2.6 | 276.8 ± 12.7 | 444.4 ± 32.0 | 130.7 ± 12.7 | 194.0 ± 15.4 | 334.5 ± 16.7 |
| | −4 | 6.15 ± 0.18 | 1.64 ± 0.10 | 65.2 ± 2.7 | 79.2 ± 2.9 | 26.4 ± 2.7 | – | – | – | – | – | 4.9 ± 1.5 | 307.9 ± 28.4 | 456.1 ± 11.6 | 174.5 ± 13.6 | 191.2 ± 18.7 | 304.2 ± 13.3 |
| | −5 | 6.20 ± 0.35 | 1.72 ± 0.06 | 82.8 ± 2.1 | 88.1 ± 5.3 | 44.6 ± 2.6 | – | – | – | – | – | 10.9 ± 0.9 | 298.7 ± 22.3 | 570.0 ± 40.4 | 27.2 ± 20.3 | 194.4 ± 11.0 | 358.0 ± 19.4 |
| Untreated with AMC & DO > 6 mg L$^{-1}$ | −1 | 6.05 ± 0.11 | 1.73 ± 0.03 | 64.9 ± 5.3 | 45.3 ± 1.1 | 54.9 ± 2.9 | 0.001 | 0.62 ± 0.05 | 36.4 ± 1.4 | 2.78 ± 0.08 | 14.3 ± 0.96 | 9.1 ± 3.5 | 301.1 ± 9.4 | 471.5 ± 15.6 | 143.1 ± 13.3 | 222.7 ± 16.0 | 347.9 ± 13.5 |
| | −2 | 5.48 ± 0.27 | 1.38 ± 0.05 | 76.7 ± 6.0 | 30.6 ± 2.0 | 50.5 ± 2.0 | – | – | – | – | – | 6.5 ± 2.4 | 280.4 ± 21.6 | 577.4 ± 11.3 | 249.6 ± 25.6 | 213.7 ± 11.6 | 430.1 ± 17.5 |
| | −3 | 5.61 ± 0.42 | 1.74 ± 0.07 | 69.8 ± 4.1 | 70.2 ± 0.8 | 43.0 ± 1.4 | – | – | – | – | – | 11.4 ± 2.1 | 252.0 ± 19.7 | 621.7 ± 24.3 | 44.1 ± 15.4 | 246.6 ± 18.7 | 393.7 ± 23.4 |
| | −4 | 5.55 ± 0.47 | 1.49 ± 0.12 | 79.7 ± 3.9 | 20.9 ± 0.6 | 46.6 ± 1.6 | – | – | – | – | – | 9.1 ± 2.3 | 264.3 ± 16.3 | 513.5 ± 26.3 | 144.3 ± 8.8 | 218.0 ± 22.0 | 321.1 ± 15.2 |
| | −5 | 5.21 ± 0.28 | 1.17 ± 0.01 | 85.3 ± 2.4 | 71.8 ± 3.4 | 46.1 ± 3.8 | – | – | – | – | – | 9.6 ± 2.3 | 247.9 ± 10.0 | 641.7 ± 30.9 | 118.9 ± 6.3 | 188.6 ± 17.9 | 342.5 ± 10.0 |
| Treated with AMC & DO > 6 mg L$^{-1}$ | −1 | 6.26 ± 0.35 | 1.25 ± 0.03 | **98.5 ± 5.5** | 35.9 ± 1.6 | 47.9 ± 0.9 | 0.001 | 0.12 ± 0.02 | 25.6 ± 2.7 | 1.51 ± 0.07 | 19.1 ± 2.04 | 9.8 ± 0.8 | 190.3 ± 6.3 | 460.5 ± 22.1 | 88.7 ± 5.1 | 167.7 ± 9.9 | 291.4 ± 19.2 |
| | −2 | 6.27 ± 0.35 | 1.85 ± 0.05 | 78.6 ± 3.9 | 44.9 ± 1.5 | 47.1 ± 1.6 | – | – | – | – | – | 7.1 ± 2.0 | 193.4 ± 15.2 | 518.3 ± 16.4 | 59.5 ± 12.6 | 173.3 ± 16.4 | 322.3 ± 11.8 |
| | −3 | 6.43 ± 0.27 | 1.83 ± 0.04 | 61.1 ± 4.2 | 85.1 ± 4.8 | 51.0 ± 2.5 | – | – | – | – | – | 8.7 ± 1.6 | 198.7 ± 7.7 | 444.9 ± 23.3 | 195.1 ± 30.0 | 173.6 ± 15.2 | 321.4 ± 14.2 |
| | −4 | 6.03 ± 0.52 | 1.81 ± 0.07 | 68.1 ± 3.4 | 44.6 ± 1.3 | 41.8 ± 1.9 | – | – | – | – | – | 6.4 ± 0.4 | 216.3 ± 19.1 | 503.5 ± 45.6 | 126.6 ± 21.5 | 187.2 ± 13.8 | 312.4 ± 10.7 |
| | −5 | 5.92 ± 0.29 | 1.70 ± 0.08 | 74.6 ± 0.8 | 83.3 ± 4.3 | 44.5 ± 2.2 | – | – | – | – | – | 9.2 ± 0.9 | 225.2 ± 13.4 | 549.6 ± 28.8 | 73.6 ± 17.4 | 190.4 ± 10.7 | 324.5 ± 14.6 |

Al and Ca) and various P forms of the sediments in the surface layer from 0 to 5 cm. In the Hongfeng, sediments had high contents of TOC, Fe, Al and TP, and their mean concentrations were 5.97% (5.21%–6.43%), 43.4 g kg$^{-1}$ (26.4–54.9 g kg$^{-1}$), 75.2 g kg$^{-1}$ (52.5–106.7 g kg$^{-1}$) and 1465.1 mg kg$^{-1}$ (1208.4–1757.7 mg kg$^{-1}$), respectively. Fe-Mn hydroxide-bound Fe and residual Fe constituted the two main forms of sediment Fe and respectively accounted for 65.9% and 30.5% of the total Fe content (Table 1). Al-P and Fe-P constituted the main forms of sediment P and respectively accounted for 36.7% and 18.5% of TP (Table 1). The contents of TS and Ca in sediments ranged from 1.17% to 1.89% (mean: 1.59%) and from 20.9 g kg$^{-1}$ to 88.1 g kg$^{-1}$ (mean: 53.1 g kg$^{-1}$), respectively. Under the condition of DO < 1 mg L$^{-1}$, after aluminum modification, the Al content and P forms of the sediments in the 1 cm surface layer notably varied. The Al and Al-P contents of this sediment layer respectively reached 97.6 ± 4.6 g kg$^{-1}$ and 542.7 ± 24.9 mg kg$^{-1}$ and were obviously higher than those of lower sediments. Under the condition of DO > 6 mg L$^{-1}$, after aluminum modification, the Al content of the sediments in the 1 cm surface layer also increased and reached 98.5 ± 5.5 g kg$^{-1}$; however, the Al-P content of this sediment layer did not experience any obvious variation.

## 4. Discussion

### 4.1. Immobilization capacity of AMC on sediment P

To quantitatively assess the capacity of AMC for immobilizing sediment P, the internal P input fluxes of the experimental group and the control group were calculated by two methods (Table 2). The first method was based on the variations in the SRP concentration of overlying water in cores over time. According to the results, under anaerobic incubation conditions not dosed with AMC, the internal P input flux of sediments was the highest and reached 13.26 ± 1.20 mg m$^{-2}$ d$^{-1}$. After dosing with AMC, the concentration of SRP in overlying water maintained a low level (0.025–0.047 mg L$^{-1}$; Fig. 2a), suggesting that internal P release had obviously been inhibited. In this case, internal P input fluxes were only 0.54 ± 0.03 mg m$^{-2}$ d$^{-1}$. Under aerobic conditions, both with and without AMC dosage, the SRP concentration of overlying water in cores uniformly presented a slight declining trend (Fig. 2b), suggesting that sediment P had not been released and that the P in overlying water experienced sedimentation. In this case, internal P input fluxes were −0.31 ± 0.04 mg m$^{-2}$ d$^{-1}$ (treated with AMC) and −0.66 ± 0.15 mg m$^{-2}$ d$^{-1}$ (not treated with AMC). The second method was based on the P concentration gradient at the SWI and Fick's first law. To be specific, under anaerobic incubation conditions not dosed with AMC, because of intense release, the soluble P concentration gradient at the SWI had vanished (Fig. 3). Thus, this method is not available for the calculation of release flux in such samples. In other incubated cores, internal P input fluxes were uniformly low at 0.22 mg m$^{-2}$ d$^{-1}$ (DO < 1 mg L$^{-1}$; treated with AMC), 0.06 mg m$^{-2}$ d$^{-1}$ (DO > 6 mg L$^{-1}$; treated with AMC) and 0.07 mg m$^{-2}$ d$^{-1}$ (DO > 6 mg L$^{-1}$; untreated with AMC). Because of their different principles, the results calculated by the two methods showed small differences but they reflected that sediment P would experience intense release under anaerobic conditions and that its release under aerobic conditions would be weak.

In this study, sediment P release occurred only under anaerobic conditions, similar to the findings of previous studies (Mortimer, 1941; McManus et al., 1997). Under anaerobic conditions, the dosing of AMC caused internal P input flux to decline from 13.26 ± 1.20 mg m$^{-2}$ d$^{-1}$ to 0.54 ± 0.03 mg m$^{-2}$ d$^{-1}$, with a declining rate of 95.9%. In this case, the removal rate of SRP from

**Table 2**
The release flux of P from sediment, calculated based on the variation of P concentrations in the overlying water, under different treatment conditions. Positive fluxes are out of sediment.

| Treatment | Sediment P release flux (mg $m^{-2}$ $d^{-1}$) | |
|---|---|---|
| | Calculation based on the variations in the P concentration of overlying water over time | Calculation based on the P concentration gradient at the SWI and Fick's first law. |
| Treated with AMC & DO < 1 mg $L^{-1}$ | 0.54 ± 0.03 | 0.22 |
| Untreated with AMC & DO < 1 mg $L^{-1}$ | 13.26 ± 1.20 | n/a |
| Treated with AMC & DO > 6 mg $L^{-1}$ | −0.31 ± 0.04 | 0.06 |
| Untreated with AMC & DO > 6 mg $L^{-1}$ | −0.66 ± 0.15 | 0.07 |

overlying water reached 90.31% (Fig. 2a), suggesting that AMC had a strong capacity of immobilizing sediment P. Under aerobic conditions, sediment P release was obviously inhibited, in which case it was unnecessary to dose with AMC or other inactivating agents for internal P input control.

### 4.2. Mechanism of internal P loading reduction by AMC

Under aerobic conditions, oxygen is allowed to penetrate through the SWI until reaching a depth of several millimeters below the surface layer of sediments, thus forming a thin oxide layer. According to the classic redox zoning theory, in this oxide layer, Fe mainly exists in oxidized forms (such as Fe oxides and hydroxides) (Froelich et al., 1979; Och et al., 2012). These oxidized Fe compounds have large specific surface areas and strong ion absorption capacities (Nóbrega et al., 2014). In the Hongfeng, surface sediments had a high Fe content, averaging 43.4 g $kg^{-1}$ (Table 1). Thus, when overlying water was in an aerobic state, this thin oxide layer on the outermost surface of sediments (usually above 10 mm) naturally formed an inactivation layer similar to Fe salts. In this case, it would be difficult for SRP to pass through this oxidized Fe salt layer and enter overlying water (Fig. 3c and d). On the contrary, when overlying water was in an anaerobic state, the clay layer had a low redox potential and $Fe^{3+}$ was reduced into $Fe^{2+}$, accompanied by the reductive dissolution of Fe-P in sediments. Considering that Fe-P constituted one of the main forms of sediment P in the Hongfeng (with a mean concentration of 271.8 mg $kg^{-1}$, Table 1), if no inactivating agent coverage was adopted, the large amount of free-state SRP formed by the reductive dissolution of Fe-P would penetrate the SWI and cause SRP in overlying water to rise intensely (Fig. 3a and b). This coincided with our observations of the variations in the SRP concentration of overlying water (Fig. 2). According to the correlation analysis, first, the SRP and soluble Fe from the sediments of the Hongfeng presented a significant positive correlation ($P < 0.01$, Fig. 5), which further confirmed the role of the reductive dissolution of Fe-P as the main mechanism of sediment P release (Ding et al., 2016). Second, in an anaerobic environment, the microorganisms in sediments utilized sulfate radicals as electron acceptors to generate $H_2S$ (Fig. 4), and could promote the precipitation of Fe (FeS) and further facilitate the dissolution of Fe-P. That is to say, sulfate reduction was coupled with Fe reduction to promote sediment P release (Ding et al., 2012).

In this study, AMC was dosed onto the sediment surface and

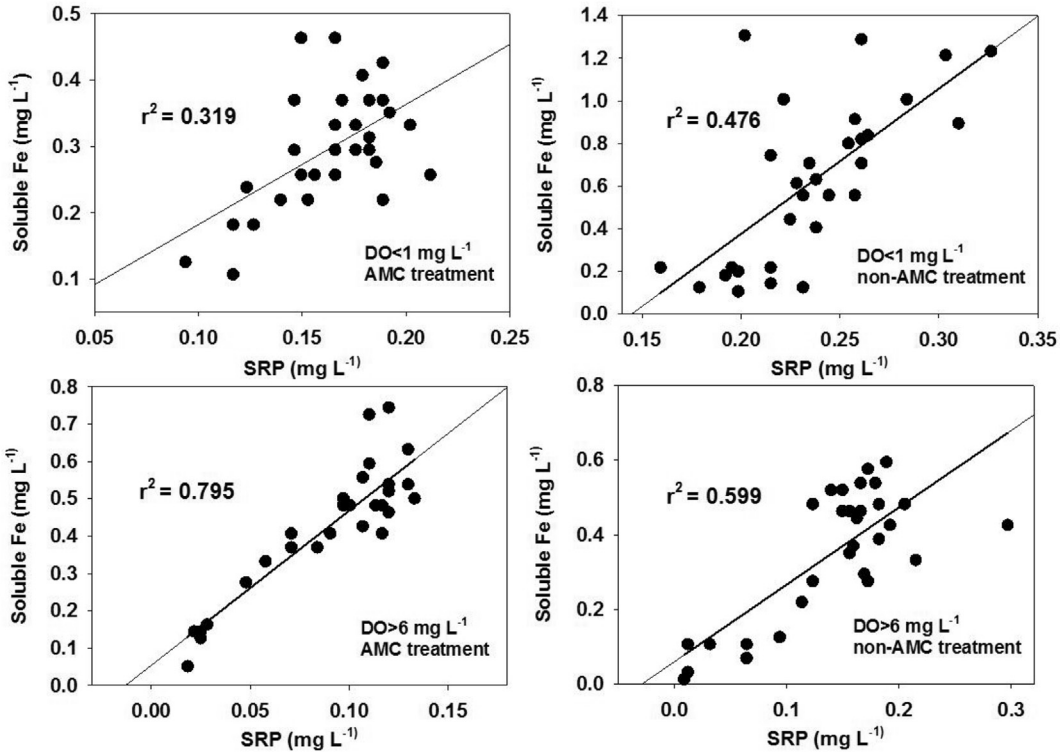


**Fig. 5.** Correlation between SRP and soluble Fe concentrations in the treated and untreated sediments with AMC under different oxidation states.

powerfully inhibited labile P in pore water from entering water even under anaerobic conditions (Fig. 2a). Under anaerobic conditions, SRP and labile P had very high concentration gradients at the SWI (Fig. 3a and b), pointing to a strong diffusion of phosphate radicals from sediments to overlying water. However, when the inactivating agent was dosed onto the sediment surface, the concentrations of SRP and labile P in the AMC capping layer both dropped abruptly to low levels (0.015 mg $L^{-1}$ and 0.038 mg $L^{-1}$ on average, respectively). This is because the $Al_2(SO_4)_3$ component in AMC played a vital role. That is, after $Al_2(SO_4)_3$was hydrolyzed and generated $Al(OH)_3$, the huge specific surface area strongly adsorbed phosphates and formed Al-P, thus creating a barrier at a depth of several millimeters above the SWI and blocking the phosphate exchange between pore water and overlying water in sediments. In lake sediments, the inorganic P combined with Al is highly stable and such combination is permanent (Rydin and Welch, 1999). Thus, AMC can stably immobilize the upward-migrating labile P from sediment pore water. Furthermore, the immobilization of phosphates by AMC and other aluminum-salt inactivating agents is not influenced by variations in redox conditions, which constitutes an advantage not enjoyed by iron-salt inactivating agents (Rydin and Welch, 1999; Rydin, 2000).

Because of the AMC dosing, the $Al_2(SO_4)_3$ in the inactivating agents partially dissolved and was released into pore water and overlying water. As a result, the $Al^{3+}$ and $SO_4^{2-}$ concentrations in the water of incubated cores and in the pore water of outermost surface sediments both increased to some extent (Table S1). To be specific, a high $SO_4^{2-}$ concentration could increase the intensity of sulfate reduction, enhance the co-precipitation of reduced S ($H_2S$) and $Fe^{2+}$ in sediments, and promote the reductive dissolution of Fe-P, which would be unfavorable for the immobilization of sediment P (Caraco et al., 1993; Rozan et al., 2002). In the incubation experiment, the $SO_4^{2-}$ concentration of the 1 cm surface layer was only observed, so it was impossible to judge whether the $SO_4^{2-}$ generated by the dissolution of AMC would penetrate into the sediment pore water below the AMC coverage layer and further exert some influence on the geochemical cycle of Fe-P. However, this process needs close attention.

Aluminum-salt inactivating agents have a strong P adsorption capacity and is thought to be the main mechanism for inhibiting sediment P release (Rydin, 2000). However, there is little knowledge available about the reaction between aluminum salts and sediment P. In this study, the thin layer coverage based on AMC could provide a labile barrier system for inhibiting the P flux from sediments. In AMC, labile Al reacted with the SRP released from sediments and formed inert Al-P. This role was similar to the function of the Fe oxide layer under aerobic conditions. Unaffected by variations in redox conditions, the immobilized P had a higher stability. In short, surface adsorption reaction constituted the main mechanism of the immobilization of the internal P from sediments by AMC. This discovery is of great significance for the applications of aluminum-salt inactivating agents.

### 4.3. Factors affecting the application of AMC in lake restoration

The ratio of labile P composition content to TP content in sediments is the main factor influencing the use rate of inactivating agents. According to the study conducted by Malecki-Brown et al. (2009), it took 0.28 mg $Al^{3+}$ to immobilize 1 mg $PO_4^{3-}$; however, because of the competition between sediment components (such as organic matter) and $PO_4^{3-}$ for adsorptive sites on the surface of $Al(OH)_3$, the use rate of $Al^{3+}$ must be increased to achieve the goal of controlling sediment P release. Rydin and Welch (1998) held that the dosing rate of aluminum salts should be based to a great extent on the content of Fe-P in sediments, mainly because of the sensitivity of Fe-P to redox conditions and its susceptibility to release. The study done by Pilgrim et al. (2007) indicated that, when setting Al:P at 4:1 (atomic ratio), the use rate could fully inactivate the releasable P in surface sediments. Kopáček et al. (2005) investigated 43 lakes of different nutritional conditions, pH values, climatic conditions and P input conditions, and the results showed that, when $Al_{NaOH\text{-}25}$:$Fe_{BD} > 3$ or $Al_{NaOH\text{-}25}$:$P_{(H2O+BD)} > 25$, the release of sediment P could be effectively controlled, even in an anaerobic environment. Considering the complexity of sediment composition and P cycle, in this study, the optimal dosage of AMC (180 g $m^{-2}$) was determined according to a series of dosage tests. Seen from the inactivation effect, this dosage could achieve a relatively ideal effect of internal P input control.

The timing of dosing inactivating agents is one of the most important factors to be considered in conducting internal P pollution control engineering. In lakes, sediment P is usually released on a seasonal basis. According to the study conducted by Steinman et al. (2009) on Lake Mona, during the spring, sediment P release was about 9% of TP, whereas in the summer and early autumn, it could reach as high as 68%–82%. The study done by Churchill et al. (2009) found that inactivation had the worst control effect in the winter and that it might even increase the release of nutrient substances. Generally, from late spring to early autumn, the SWI has a high temperature, so biological activities are obviously strengthened, which further facilitates the conversion of organic P into inorganic P. In addition, at this point, the sediment surface is usually anoxic, which intensifies the reductive dissolution of Fe-P. It is thus clear that this period has the highest internal P input and that it is an ideal period for inactivation engineering.

Aluminum-salt inactivating agents, through forming a coverage layer on the surface layer of sediments and reducing sediment P release, can have an effective time of 10–15 years (Cooke et al., 1993; Rydin, 2000; Berkowitz et al., 2006; Malecki-Brown et al., 2009). The sustainability of their inactivation effect mainly depends on temporal variations in the adsorptive capacity of $Al(OH)_3$, and adsorptive capacity is in direct proportion to the surface area of inactivating agents. With the passage of time, $Al(OH)_3$ gradually forms gibbsite, and results in the reduction of surface area (Berkowitz et al., 2006). Furthermore, the binding between sediment components (such as inorganic matter) also reduces surface area and thus affects the sustainability of the inactivation effect (Borggaard et al., 1990). In addition, the re-suspension capacity of $Al(OH)_3$ floccule is five times of that of ordinary sediments (Egemose et al., 2009); therefore, AMC is susceptible to the influence of storm waves, which further weakens the inactivation effect. In shallow lakes with an intense action of storm waves, it is necessary to assess their inactivation effect, especially with respect to stability. The pH of water is another key factor affecting the inactivating efficiency of aluminum salts. Hydrolysis of aluminium salts usually occurs only in a weak alkaline condition, with an optimal pH range of 6–8 (Haggard et al., 2005; Lin et al., 2017). The hydrolysate can strongly adsorb phosphate, which is the key to inactivating P in sediments. This also limits the application of inactivating agents for aluminum salts in weak alkaline waters.

Inactivating agents for aluminum salts have a strong capacity for immobilizing sediment P and are extensively applied to lake restoration after pollution by internal P. However, dosing inactivating agents that containing aluminum salts into water may result in chemical pollution (such as excessive dissolved Al). In our study, after the addition of AMC, the concentration of aluminum ions increased slightly in overlying water (from 8.5 μg $L^{-1}$ to 23 μg $L^{-1}$) and in pore water (from 18 μg $L^{-1}$ to 43 μg $L^{-1}$) during the incubation (Table S1). However, its concentration is still far below the limit of drinking water sanitary standard in China (200 μg $L^{-1}$;

GB5749-2006). This result indicates that the environmental risk of AMC is acceptable.

P release from sediments occurs mainly under anoxic conditions, but hardly under aerobic conditions (Fig. 2a and b). Therefore, the remediation of P pollution in sediments is necessary in lakes with long-term or seasonal hypoxia. The DO levels and its distributions in waters are determined by several factors, among which water depth and water nutrient level are usually the most important ones. The bottom water of deep and eutrophic lakes or reservoirs is often observed to be chronically or seasonally hypoxic. Our research indicates that AMC is effective in controlling sediment P input under anoxic conditions. Therefore, AMC can be an effective remediation material in deep eutrophic lakes or reservoirs. In field applications, the dosage, dosing timing, lake characteristics (pH and disturbance by storm waves) and other factors of AMC may all influence the effectiveness and sustainability of inactivating agents, thus, further in-depth studies are needed.

## 5. Conclusion

Under aerobic conditions, there was no obvious sediment P release, irrespective of AMC dosing. Under anaerobic conditions, AMC effectively reduces the release flux of sediment SRP. According to high-resolution sampling, there was a positive correlation between soluble Fe and SRP in pore water, suggesting that the reductive dissolution of Fe-P constituted the main mechanism of sediment P release. After dosing AMC, the concentrations of SRP and labile P in the capping layer both dropped abruptly to low levels even under anaerobic conditions. This is because AMC had strongly adsorbed phosphates, formed inert Al-P, and thus created a barrier on the sediment surface and blocked phosphate exchange between pore water and overlying water in sediments. The immobilization of phosphates by AMC was not influenced by variations in redox conditions; therefore, the immobilized P had better stability. In this case, AMC can be an effective inactivating agent for remediation of internal P pollution in deep eutrophic reservoirs.

## Acknowledgements

This study was sponsored jointly by CAS Interdisciplinary Innovation Team of China, the Chinese NSF project (No. 41773145), the National Key Research and Development Project by MOST of China (No. 2016YFA0601000), and the Science and Technology Project of Guizhou Province, China ([2013]2281, [2015]2001 and [2016]2802).

## Appendix A. Supplementary data

Supplementary data to this article can be found online at https://doi.org/10.1016/j.chemosphere.2018.10.095.

## References

Berkowitz, J., Anderson, M.A., Amrhein, C., 2006. Influence of aging on phosphorus sorption to alum flock in lake water. Water Res. 40, 911–916.
Borggaard, O.K., Jorgensen, S.S., Moberg, J.P., Raben-Lange, B., 1990. Influence of organic matter on phosphate adsorption by aluminum and iron oxides in sandy soils. Eur. J. Soil Sci. 41, 443–449.
Campanella, L., D'Orazio, D., Petronio, B.M., Pietrantonio, E., 1995. Proposal for a metal speciation study in sediments. Anal. Chim. Acta 309, 387–393.
Caraco, N.F., Cole, J.J., Likens, G.E., 1993. Sulfate control of phosphorus availability in lakes - a test and reevaluation of Hasler and Einsele model. Hydrobiologia 253, 275–280.
Carpenter, S.R., 2005. Eutrophication of aquatic ecosystems: bistability and soil P. Proc. Natl. Acad. Sci. 102, 10002–10005.
Chen, M., Cui, J., Lin, J., Ding, S., Gong, M., Ren, M., Tsang, D.C.W., 2018. Successful control of internal phosphorus loading after sediment dredging for 6 years: a field assessment using high-resolution sampling techniques. Sci. Total Environ. 927, 616–617.
Churchill, J.J., Beutel, M.W., Burgoon, P.S., 2009. Evaluation of optional dose and mixing regime for alum treatment of Matthiesen Creek inflow to Jameson Lake, Washington. Lake Reservoir Manag. 25, 102–110.
Conley, D.J., Paerl, H.W., Howarth, R.W., Boesch, D.F., Seitzinger, S.P., Havens, K.E., Lancelot, C., Likens, G.E., 2009. Controlling eutrophication: nitrogen and phosphorus. Science 323, 1014–1015.
Cooke, G.D., Welch, E.B., Martin, A.B., Fulmer, D.G., Hyde, J.B., Schrieve, G.D., 1993. Effectiveness of Al, Ca, and Fe salts for control of internal phosphorus loading in shallow and deep lakes. Hydrobiologia 253, 323–335.
Dai, L., Pan, G., 2014. The effects of red soil in removing phosphorus from water column and reducing phosphorus release from sediment in Lake Taihu. Water Sci. Technol. 69, 1052–1058.
Davlson, W., Zhang, H., 1994. *In situ* speciation measurements of trace components in natural waters using thin-film gels. Nature 367, 546–548.
Ding, S., Chen, M., Cui, J., Wang, D., Lin, J., Zhang, C., Tsang, D.C.W., 2018b. Reactivation of phosphorus in sediments after calcium-rich mineral capping: implication for revising the laboratory testing scheme for immobilization efficiency. Chem. Eng. J. 331, 720–728.
Ding, S., Chen, M., Gong, M., Fan, X., Qin, B., Xu, H., Gao, S., Jin, Z., Tsang, D.C.W., Zhang, C., 2018a. Internal phosphorus loading from sediments causes seasonal nitrogen limitation for harmful algal blooms. Sci. Total Environ. 625, 872–884.
Ding, S., Sun, Q., Chen, X., Liu, Q., Wang, D., Lin, J., Zhang, C., Tsang, D.C.W., 2018c. Synergistic adsorption of phosphorus by iron in lanthanum modified bentonite (Phoslock®): new insight into sediment phosphorus immobilization. Water Res. 134, 32–43.
Ding, S., Sun, Q., Xu, D., Jia, F., He, X., Zhang, C., 2012. High-resolution simultaneous measurements of dissolved reactive phosphorus and dissolved sulfide: the first observation of their simultaneous release in the sediments. Environ. Sci. Technol. 46, 8297–8304.
Ding, S., Wang, Y., Xu, D., Zhu, C., Zhang, C., 2013. Gel-based coloration technique for the submillimeter-scale imaging of labile phosphorus in the sediments and soils with diffusive gradients in thin films. Environ. Sci. Technol. 47, 7821–7829.
Ding, S., Yan, W., Dan, W., Yang, Y.L., Gong, M., Zhang, C., 2016. *In situ*, high-resolution evidence for iron-coupled mobilization of phosphorus in sediments. Sci. Rep. 6, 24341.
Ding, S.M., Han, C., Wang, Y.P., Yao, L., Xu, D., Sun, Q., Williams, P.N., Zhang, C.S., 2015. *In situ*, high-resolution imaging of labile phosphorus in sediments of a large eutrophic lake. Water Res. 74, 100–109.
Douglas, G.B., Adeney, J.A., Robb, M., 1999. A novel technique for reducing bioavailable phosphorus in water and sediments. In: Proceeding of the International Association Water Quality Conference on Diffuse Pollution, pp. 517–523.
Egemose, S., Wauer, G., Kleeberg, A., 2009. Resuspension behavior of aluminum treated lake sediments: effects of ageing and pH. Hydrobiologia 636, 203–217 . .
Fisher, M.M., Reddy, K.R., 2001. Phosphorus flux from wetland soils affected by long term nutrient loading. J. Environ. Qual. 30, 261–271.
Frankowski, L., Bolaiek, J., Szostek, A., 2002. Phosphorus in bottom sediments of pomeranian bay (Southern Baltic-Poland). Estuar. Coast Shelf Sci. 54, 1027–1038.
Froelich, P.N., Klinkhammer, G.P., Bender, M.L., Luedtke, N.A., Heath, G.R., Cullen, D., Dauphin, P., Hammond, D., Hartman, B., Maynard, V., 1979. Early oxidation of organic matter in pelagic sediments of the eastern equatorial Atlantic: suboxic diagenesis. Geochim. Cosmochim. Ac. 43, 1075–1090.
Gao, Y., Cornwell, J.C., Stoecker, D.K., Owens, M.S., 2015. Influence of cyanobacteria blooms on sediment biogeochemistry and nutrient fluxes. Limnol. Oceanogr. 59, 959–971.
Haggard, B.E., Moore, P.A., Delaune, P.B., 2005. Phosphorus flux from bottom sediments in lake Eucha, Oklahoma. J. Environ. Qual. 34, 724–728.
Huang, L., Li, Z., Bai, X., Li, R.Y., Wu, H., Wei, D., Yu, L., 2016. Laboratory study of phosphorus retention and release by eutrophic lake sediments: modeling and implications for P release assessments. Ecol. Eng. 95, 438–446.
Hupfer, M., Gaechter, R., Giovanoli, R., 1995. Transformation of phosphorus species in settling seston and during early sediment diagenesis. Aquat. Sci. 57, 305–324.
Huser, B.J., Pilgrim, K.M., 2014. A simple model for predicting aluminum bound phosphorus formation and internal loading reduction in lakes after aluminum addition to lake sediment. Water Res. 53, 378–385.
Immers, A.K., Vendrig, K., Ibelings, B.W., Van Donk, E., Ter Heerdt, G.N.J., Geurts, J.J.M., Bakker, E.S., 2014. Iron addition as a measure to restore water quality: implications for macrophyte growth. Aquat. Bot. 116, 44–52.
Kopáček, J., Borovec, J., Hejzlar, J., Ulrich, K., Norton, S., Amirbahman, A., 2005. Aluminum control of phosphorus sorption in lake sediments. Environ. Sci. Technol. 39, 8784–8789.
Lavery, P.S., Oldham, C.E., Ghisalberti, M., 2001. The use of Fick's First Law for predicting porewater nutrient fluxes under diffusive conditions. Hydrol. Process. 15, 2435–2451.
Li, C., Yu, H., Tabassum, S., Li, L., Wu, D., Zhang, Z., Kong, H., Xu, P., 2017. Effect of calcium silicate hydrates on phosphorus immobilization and speciation in shallow lake sediment. Chem. Eng. J. 317, 844–853.
Li, Y.H., Gregory, S., 1974. Diffusion of ions in sea-water and in deep-sea sediments. Geochim. Cosmochim. Ac 38, 703–714.
Lin, J., Sun, Q., Ding, S., Wang, D., Wang, Y., Chen, M., Shi, L., Fan, X., Tsang, D.C.W., 2017. Mobile phosphorus stratification in sediments by aluminum immobilization. Chemosphere 186, 644–651.

Lin, J., Jiang, B., Zhan, Y., 2018. Effect of pre-treatment of bentonite with sodium and calcium ions on phosphate adsorption onto zirconium-modified bentonite. J. Environ. Manag. 217, 183–195.
Lin, J.W., He, S.Q., Zhang, H.H., Zhan, Y.H., Zhang, Z.B., 2019. Effect of zirconium-modified zeolite addition on phosphorus mobilization in sediments. Sci. Total Environ. 646, 144–157.
Malecki-Brown, L.M., White, J.R., Sees, M., 2009. Alum application to improve water quality in a municipal wastewater treatment wetland. J. Environ. Qual. 38, 814–821.
McManus, J., Berelson, W.M., Coale, K.H., Johnson, K.S., Kilgore, T.E., 1997. Phosphorus regeneration in continental margin the sediment. Geochim. Cosmochim. Ac. 61, 2891–2907.
Mortimer, C.H., 1941. The exchange of dissolved substances between mud and water in lakes. J. Ecol. 29, 280–329.
Murphy, J., Riley, J.P., 1962. A modified single solution method for the determination of phosphate in natural waters. Anal. Chim. Acta 27, 31–36.
Nausch, M., Nausch, G., Lass, H.U., Mohrholz, V., Nagel, K., Siegel, H., Wasmund, N., 2009. Phosphorus input by upwelling in the Eastern Gotland Basin (Baltic Sea) in summer and its effects on filamentous cyanobacteria. Estuar. Coast Shelf Sci. 83, 434–442.
Nóbrega, G.N., Otero, X.L., Macias, F., Ferreira, T.O., 2014. Phosphorus geochemistry in a Brazilian semiarid mangrove soil affected by shrimp farm effluents. Environ. Monit. Assess. 186, 5749–5762.
Och, L.M., Müller, B., Voegelin, A., Ulrich, A., Göttlicher, J., Steiniger, R., Mangold, S., Vologina, E.G., Sturm, M., 2012. New insights into the formation and burial of Fe/Mn accumulations in Lake Baikal sediments. Chem. Geol. 330–331, 244–259.
Penn, M.R., Auer, M.T., Doerr, S.M., Driscoll, C.T., Brooks, C.M., Effler, S.W., 2000. Seasonality in phosphorus release rates from the sediments of a hypereutrophic lake under a matrix of ph and redox conditions. Can. J. Fish. Aquat. Sci. 57, 1033–1041.
Pilgrim, K.M., Huser, B.J., Brezonik, P.L., 2007. A method for comparative evaluation of whole-lake and inflow alum treatment. Water Res. 41, 1215–1224.
Qin, B., Zhu, G., Zhang, L., Luo, L., Gao, G., Binhe, G.U., 2006. Estimation of internal nutrient release in large shallow Lake Taihu, China. Sci. China, Ser. A D. 49, 38–50.
Reitzel, K., Hansen, J., Andersen, F.O., Hansen, K.S., Jensen, H.S., 2005. Lake restoration by dosing aluminum relative to mobile phosphorus in the sediment. Environ. Sci. Technol. 39, 4134–4140.
Rozan, T.F., Taillefert, M., Trouwborst, R.E., Glazer, B.T., Ma, S., Herszage, J., Valdes, L.M., Price, K.S., Luther III, G.W., 2002. Iron-sulfur-phosphorus cycling in the sediments of a shallow coastal bay: implications for sediment nutrient release and benthic macroalgal blooms. Limnol. Oceanogr. 47, 1346–1354.
Rydin, E., Welch, E.B., 1998. Aluminum dose required to inactivate phosphate in lake sediments. Water Res. 32, 2969–2976.
Rydin, E., 2000. Potentially mobile phosphorus in Lake Erken sediment. Water Res. 34, 2037–2042.
Rydin, E., Welch, E.B., 1999. Dosing alum to Wisconsin lake sediments based on in vitro formation of aluminum bound phosphate. Lake Reservoir Manag. 15, 324–331.
Søndergaard, M., Jensen, J.P., Jeppesen, E., 2003. Role of sediment and internal loading of phosphorus in shallow lakes. Hydrobiologia 506, 135–145.
Steinman, A., Chu, X., Ogdahl, M., 2009. Spatial and temporal variability of internal and external phosphorus loads in Mona Lake, Michigan. Aquat. Ecol. 43, 1–18.
Su, Y., Cui, H., Li, Q., Gao, S., Shang, J.K., 2013. Strong adsorption of phosphate byamorphous zirconium oxide nanoparticles. Water Res. 47, 5018–5026.
Tamura, H., Goto, K., Yotsuyanagi, T., Nagayama, M., 1974. Spectrophotometric determination of iron(III) with 1, 10-phenanthroline in the presence of large amounts of iron(III). Talanta 21, 314–318.
Tessier, A., Campbell, P.G., Bisson, M., 1979. Sequential extraction procedure for the speciation of particulate trace metals. Anal. Chem. 51, 844–851.
Ullman, W.J., Aller, R.C., 1982. Diffusion coefficients in nearshore marine sediments. Limnol. Oceanogr. 27, 552–556.
Vopel, K., Gibbs, M., Hickey, C.W., Quinn, J., 2008. Modification of sediment-water solute exchange by sediment-capping materials: effects on $O_2$ and pH. Mar. Freshw. Res. 59, 1101–1110.
Wang, J.F., Chen, J.A., Christopher, D., Yang, H.Q., Dai, Z.H., 2015. Spatial distribution, fractions and potential release of sediment phosphorus in the Hongfeng Reservoir, southwest China. Lake Reservoir Manag. 31, 214–224.
Wang, J.F., Chen, J.A., Ding, S.M., Guo, J.Y., Christopher, D., Dai, Z.H., Yang, H.Q., 2016. Effects of seasonal hypoxia on the release of phosphorus from sediments in deep-water ecosystem: a case study in Hongfeng Reservoir, southwest China. Environ. Pollut. 219, 858–865.
Wang, Y., Ding, S., Wang, D., Sun, Q., Lin, J., Shi, L., Chen, M., Zhang, C., 2017. Static layer: a key to immobilization of phosphorus in sediments amended with lanthanum modified bentonite (Phoslock®). Chem. Eng. J. 325, 49–58.
Xiao, R., Bai, J.H., Lu, Q.Q., Zhao, Q.Q., Gao, Z.Q., Wen, X.J., Liu, X.H., 2015. Fractionation, transfer, and ecological risks of heavy metals in riparian and ditch wetlands across a 100-year chronosequence of reclamation in an estuary of China. Sci. Total Environ. 517, 66–75.
Xu, D., Chen, Y.F., Ding, S.M., Sun, Q., Wang, Y., Zhang, C.S., 2013. Diffusive gradients in thin films technique equipped with a mixed binding gel for simultaneous measurements of dissolved reactive phosphorus and dissolved iron. Environ. Sci. Technol. 47, 10477–10484.
Xu, D., Wu, W., Ding, S.M., Sun, Q., Zhang, C.S., 2012. A high-resolution dialysis technique for rapid determination of dissolved reactive phosphate and ferrous iron in pore water of sediments. Sci. Total Environ. 421–422, 245–252.
Yin, H., Zhu, J., 2016. *In situ* remediation of metal contaminated lake sediment using naturally occurring, calcium-rich clay mineral-based low-cost amendment. Chem. Eng. J. 285, 112–120.
Yu, J., Ding, S., Zhong, J., Fan, C., Chen, Q., Yin, H., Zhang, L., Zhang, Y., 2017. Evaluation of simulated dredging to control internal phosphorus release from sediments: focused on phosphorus transfer and resupply across the sediment-water interface. Sci. Total Environ. 592, 662–673.